Localization length in two-dimensional disordered systems: effects of evanescent modes

2009 J. Phys.: Condens. Matter 21 405302

(http://iopscience.iop.org/0953-8984/21/40/405302)

J. Phys.: Condens. Matter **21** (2009) 405302 (10pp) doi:10.1088/0953-8984/21/40/405302

Localization length in two-dimensional disordered systems: effects of evanescent modes

Vladimir Gasparian[1] **and Akira Suzuki**[2]

[1] Department of Physics, California State University, Bakersfield, CA 93311, USA
[2] Department of Physics, Faculty of Science, Tokyo University of Science, 1-3 Kagurazaka, Shinjyuku-ku, Tokyo 162-8601, Japan

Received 15 April 2009, in final form 26 July 2009
Published 14 September 2009
Online at stacks.iop.org/JPhysCM/21/405302

Abstract
We study the influence of evanescent modes on the scaling behavior of the renormalized localization length (RLL) in 2D disordered systems, using the δ-function potential strip model and the multichain tight-binding Anderson model. In the weak disorder regime we have evaluated the RLL for large numbers of modes M. It is shown that RLL shrinks with increasing M which indicates that the electron states will remain localized in an infinitely wide system for an arbitrarily small disorder, in agreement with existing theories. In the thermodynamic limit ($M \to \infty$) for the two models, we obtain the localization length in an infinitely large system. We show that the presence of evanescent modes enhances the RLL with respect to the value obtained when evanescent modes are absent. We also derive an exact relationship between the localization length and its corresponding average mean free path for an M-channel system for the case where propagating as well as evanescent channels are present.

1. Introduction

In quasi-one-dimensional (Q1D) and two-dimensional (2D) disordered systems the scattering boundary conditions, due to the electrons' lateral confinement, couple propagating modes to non-propagating or evanescent modes. Both of them are the solutions of Schrödinger's equation for a given energy E, but the evanescent modes decay with the distance, do not carry a current and do not contribute to the Landauer conductance of a large sample. However, these evanescent modes are of paramount importance in Q1D and 2D disordered systems because they may strongly influence the scattering matrix elements in an indirect fashion via coupling to propagating states due to the presence of impurity potentials [1–7] and due to tunneling [8]. The localization lengths (LL) are, in general, significantly larger than the values obtained when evanescent modes are absent. The effect of enhanced evanescent modes on LL was numerically studied by Cahay *et al* [9] using the scattering matrix formalism of [1]. The analogous result for LL has also been found by Heinrichs in [10], using the Anderson tight-binding (TB) model for coupled two- and three-chain systems with a white-noise potential in the weak disorder regime. Transmission, enhanced by the conversion of evanescent waves into propagating waves, was discussed in a recent article [11]. The question regarding the effect of multiple scattering of evanescent waves on the tunneling transmissivity was addressed in [12]. It was shown that the transmissivity of a 1D random system, which is periodic on average for frequencies corresponding to the gap, increases with increasing disorder when the disorder is weak enough. The evanescent modes may violate the Friedel sum rule away from the Fano resonances, even when charge is conserved, as was reported in [13]. Another reason for the growing interest in evanescent modes is due to the fact that the Rashba spin–orbit coupling strength in quantum wires couples the states along a Q1D channel with the states of transverse motion. As a consequence, evanescent modes are characterized by complex wavenumbers with real and imaginary parts. The latter can affect spin and density distributions around inhomogeneities in quantum wires [14].

In the majority of these publications, the role of evanescent modes on quantum transport has been studied in 1D or single-channel tight-binding models. 2D or multi-channel random systems with evanescent modes received much less attention [9, 10, 15, 16]. The main difficulties in 2D disordered systems arise because it is more difficult to perform analytical calculations when we deal with a large number of impurities. At present, most numerical simulations are available as one of

the effective tools to analyze the behavior of electrons in 2D and 3D systems (see, e.g., [17–19]). Therefore any study of quantum transport in disordered multi-channel systems with many impurities should be quite important and analytical results are highly desirable (see, e.g., [20, 21] and references therein). The purpose of the present work goes in this direction, in the sense that we provide analytical expressions for the RLL in the thermodynamic limit (the number of modes $M \to \infty$) for the case where propagating as well as evanescent channels are present. In the weak disorder regime we were able to obtain a closed analytic expressions for the averaged transmission and reflection coefficients for arbitrary numbers of coupled chains M. We shall establish relationships between the LL and its corresponding average mean free path for an M-channel system.

In what follows, we concentrate our attention on the weak disorder limit because this regime is of general interest for two reasons. First, in 1D and 2D systems localization occurs for arbitrarily weak potentials. Second, the LL can be evaluated in the Born approximation for an uncorrelated potential in 2D systems [15, 16, 22].

The starting point of the present work is RLL, the localization length, expressed in units of strip width, which can be defined as

$$\Lambda(w) = \frac{\xi_{L_t}(w)}{L_t}, \tag{1}$$

in analogy with single-parameter scaling for conductance [23]. Here $\xi_{L_t}(w)$ is the localization length, L_t is the width of a 2D disordered system and w represents disorder. If $\Lambda(w)$ shrinks with increasing L_t the system behaves like an insulator (the electron states will remain localized in an infinitely wide system). If it increases with L_t, the system is metallic, i.e. the electron states are extended at a large scale.

In this paper, we consider two different models which are appropriate for disordered mesoscopic systems. The first model is the set of N 2D Dirac δ potentials, distributed randomly on a strip:

$$V(x, y) = \sum_{l=1}^{N} V_l \delta(x - x_l)\delta(y - y_l), \tag{2}$$

where (x_l, y_l) denotes the position of the lth impurity in the (x, y) plane. V_l is the strength of the lth impurity potential and may be repulsive ($V_l > 0$) or attractive ($V_l < 0$).

Although the use of such an idealized model of the δ-function scatterer has some limitations, mainly when we deal with an infinite number of evanescent modes [13, 25, 26], it still allows us to get an analytical solution for many scattering problems with complicated potential configurations in 1D [27–30] as well as in 2D disordered systems [22, 31]. Note that in the case of the single δ-function scatterer ($N = 1$) the total effect of the evanescent modes can be included in the coupling constants and in this way map the multi-channel problem to the one-mode problem [13, 26]. In the general case, with two or more δ impurities, this type of simplification of the problem is not valid any more, because it is impossible to renormalize the strengths of all the δs simultaneously for a given cutoff of evanescent modes (see the appendix).

The second model is a Q1D lattice of size $L \times L_t$ described by the standard TB Hamiltonian with nearest-neighbor interaction:

$$H = \sum_i \epsilon_i |r_i\rangle\langle r_i| - t \sum_{i,j} |r_i\rangle\langle r_j|, \tag{3}$$

where ϵ_i is the energy of site i chosen randomly between $(-\frac{w}{2}, \frac{w}{2})$ with uniform probability and t is the hopping matrix element. The double sum runs over nearest neighbors. L is the length and L_t is the width of the system. The sample is connected to two semi-infinite, multi-mode leads to the left and to the right. For simplicity we take the number of modes in the left and right leads to be the same (M) and thus the width L_t of this system equals M (for a TB model the number of modes coincides with the number of sites in the transverse direction).

For these two models an analytical approach based on the characteristic determinant (the Green function poles) was developed in [22] by one of the authors (Gasparian) to find the expressions for all the scattering matrix elements in Q1D and 2D disordered systems without any restriction on the numbers of impurities and modes. In spite of the fact that the origins of these two models are quite different, they are similar in the sense that their matrix representation for the Hamiltonian operator has the same structure. This means that they can be discussed within the framework of the same approach. This proves to be useful for calculating electron average reflection and transmission coefficients, localization length and average mean free path for electrons in multi-channel systems in the weak disorder regime. In our calculations we closely follow the method proposed in [22].

This paper is organized as follows. In section 2 we discuss the randomly arranged 2D δ-function potential strip model. We briefly discuss the practical algorithm carried out in [22] for solving the Dyson equation in Q1D and 2D disordered systems without any restriction on the numbers of impurities (N) and modes (M), which leads to the description of the scattering matrix elements in terms of determinants of rank $N \times N$. In section 3 we calculate the inverse RLL for $\Lambda \ll 1$ for periodically arranged 2D δ impurities. In the thermodynamic limit $M \to \infty$ we compute the localization length in the infinitely large system. The effect of evanescent modes on the RLL is presented in section 3.1. The TB Anderson 2D model is discussed in section 4. Finally, in section 4.1 we present supplementary results for computing the localization length and average mean free path when evanescent modes are present at the Fermi level. The main conclusions are summarized in section 5. In the appendix we present the explicit forms for transmission and reflection amplitudes for the two δ-function systems and establish the relation between the Green's functions (GF) for 2D δ strip and TB models.

2. 2D strip model with randomly arranged δ impurities

Here we recall the Dyson equation for a 2D strip model with impurity δ potential, equation (2), studied in [22]. We briefly discuss the practical algorithm carried out in [22] for solving the Dyson equation in Q1D and 2D disordered systems without

any restriction on the numbers of impurities (N) and modes (M), which leads to the description of the scattering matrix elements in terms of determinants of rank $N \times N$. This will allow us to map the 2D scattering problem into a 1D problem with modified matrix elements and to obtain explicit results for RLL in the Born approximation for $\Lambda \ll 1$.

Consider the quantum transport of an electron in a 2D disordered strip, where the electron is confined in the y direction but is free to propagate in the x direction. The wavefunction of a single-electron state with energy E is described by the Schrödinger equation ($\hbar = 2m_0 = 1$):

$$\left\{-\left(\frac{\mathrm{d}^2}{\mathrm{d}x^2}+\frac{\mathrm{d}^2}{\mathrm{d}y^2}\right)+V_\mathrm{c}(y)+V(x,y)\right\}\Psi(x,y)=E\Psi(x,y), \tag{4}$$

where the confinement potential $V_\mathrm{c}(y)$ depends on the transverse direction y and $V(x,y)$ is the potential of the impurities in the 2D strip and is given by equation (2). It is worth noting that none of the main results of this paper will change drastically if, instead of the set of δ-function potentials (2), we take slightly modified δ-like potentials in each (x_l, y_l) in a 2D strip, as discussed in [3].

The transverse mode wavefunction $\chi_n(y)$ satisfies a 1D Schrödinger equation:

$$\left\{-\frac{\mathrm{d}^2}{\mathrm{d}y^2}+V_\mathrm{c}(y)\right\}\chi_n(y)=E_n\chi_n(y), \tag{5}$$

where n is the sub-band index and E_n are the sub-band energies. In general, $\chi_n(y_l)$ depends on the choice of the confinement potential $V_\mathrm{c}(y)$. If we take $V_\mathrm{c}(y)$ to be zero for $0 \leqslant y \leqslant L_t$ and infinite elsewhere, then for $\chi_n(y_l)$ we get

$$\chi_n(y_l)=\sqrt{\frac{2}{L_t}}\sin\left(\frac{n\pi y_l}{L_t}\right). \tag{6}$$

The equation for the Green's function (GF) in a Q1D system with potential $V(x,y)$ is

$$\left[-\left(\frac{\mathrm{d}^2}{\mathrm{d}x^2}+\frac{\mathrm{d}^2}{\mathrm{d}y^2}\right)+V_\mathrm{c}(y)+V(x,y)-E\right]G^{(N)}(xy;x'y') = -\delta(x-x')\delta(y-y'). \tag{7}$$

The Dyson equation for a Q1D wire can be written in the form [2, 32]

$$G^{(N)}_{nm}(x,x')=G^{(0)}_n(x,x')\delta_{nm} + \sum_{k,q}\int G^{(0)}_n(x,x'')\delta_{nk}V_{kq}(x'')G^{(N)}_{qm}(x'',x')\,\mathrm{d}x'', \tag{8}$$

where $G^{(0)}_n(x,x')$ is the GF in the absence of the defect potential $V(x,y)$ and obeys the equation

$$\left[-\frac{\mathrm{d}^2}{\mathrm{d}x^2}-(E-E_n)\right]G^{(0)}_{nm}(x;x')=-\delta(x-x')\delta_{nm}. \tag{9}$$

Thus $G^{(0)}_{nm}(x;x')$ is diagonal in the indices n and m, as $G^{(0)}_{nm}(x;x')=G^{(0)}_n(x;x')\delta_{nm}$. The explicit form of $G^0_n(x,x')$ which corresponds to a propagating mode and satisfies equation (9) is

$$G^0_n(x,x')=-\frac{\mathrm{i}}{2k_n}\exp(\mathrm{i}k_n|x-x'|), \tag{10}$$

where the wavevector k_n is given by

$$k_n=+\sqrt{E-\frac{n^2\pi^2}{L_t^2}}, \qquad n=1,2,\ldots. \tag{11}$$

The GF, $G^0_n(x,x')$, for an evanescent mode can be found from equation (10) with an analytic continuation of the $k_n = \mathrm{i}\kappa_n$, where κ_n is defined by

$$\kappa_n=+\sqrt{\frac{n^2\pi^2}{L_t^2}-E}, \qquad (E<n^2\pi^2/L_t^2). \tag{12}$$

The upper index (l) of the GF (in equation (9) the index $l = 0$) indicates that the GF is calculated in the presence of $l\delta$ potentials.

The main algorithm for finding the GF for the whole system with N δ potentials is based on the idea of recursively building up the total GF. In such calculations, the GF is evaluated first when one δ potential is available. The case of two δ potentials is then solved using the GF for a single δ potential. Then we solve the problem iteratively with N δ potentials by taking the solution with the $(N-1)$ known δs, and extract the scattering matrix elements. Thus we can obtain GF's elements in an arbitrary interval $[x_n, x_{n+1}]$ ($n = 1,\ldots,N-1$) of a disordered system [22, 28].

In the following our main interest will be in the matrix elements of the GF for the range $x, x' \leqslant x_1$. This allows us to calculate the total transmission and reflection amplitudes of an electron which is incident on the system from the left. We use the well-known relations between the scattering amplitudes and GF [33]. The explicit form of the matrix elements of GF for $x, x' \leqslant x_1$ is given as

$$G^{(N)}_{nm}(x,x')=G^{(0)}_n(x,x')\delta_{nm}+R^{(N)}_{nmL}\frac{G^0_n(x,x_1)G^0_m(x_1,x')}{\sqrt{G^0_n(x_1,x_1)G^0_m(x_1,x_1)}}, \tag{13}$$

where $R^{(N)}_{nmL}$ is the matrix element of reflection from the whole system with N δ potentials and may be written as the ratio of two determinants (for more details see [28, 30]):

$$R^{(N)}_{nmL}=(-1)^N\frac{1}{\det\,(D^{(N)}_{i,j})_{M,1}} \times \begin{vmatrix} 0 & r^{(1)}_{nm} & \cdots & r^{(N)}_{nm}\mathrm{e}^{\mathrm{i}k_n|x_N-x_1|} \\ 1 & \cdots & \cdots & \cdots \\ \vdots & \vdots & & (D^{(N)}_{i,j})_{M,m} \\ \mathrm{e}^{\mathrm{i}k_m|x_N-x_1|} & \vdots & & \end{vmatrix}. \tag{14}$$

$r^{(l)}_{nm}$ is the complex amplitude of the reflection of an electron from the isolated potential V_l in the absence of the remaining $(N-1)$ potentials [2]:

$$r^{(l)}_{nm}=\frac{V^{(l)}_{nm}\sqrt{G^{(0)}_n(x_l,x_l)G^{(0)}_m(x_l,x_l)}}{1-\sum_p^M V^{(l)}_{pp}G^{(0)}_p(x_l,x_l)}. \tag{15}$$

Note that the $r^{(l)}_{nm}$ satisfy the identity $r^{(l)}_{mm}r^{(l)}_{nn}-r^{(l)}_{mn}r^{(l)}_{nm}=0$, which can be checked directly by making use of equation (15).

The numerator of $R^{(N)}_{nmL}$ is obtained from the most significant quantity $\det(D^{(N)}_{i,j})_{M,m}$, which is the pole of the GF (see equation (16)), by augmenting it on the left and on the top. The matrix elements of the denominator $(D^{(N)}_{i,j})_{M,m}$, which contains information about the number of modes M [$1 \leqslant i, j \leqslant N$; $1 \leqslant m \leqslant M$], are

$$(D^{(N)}_{i,j})_{M,m} = -\delta_{ij} + (1-\delta_{ij}) \sum_{p=1}^{M} \frac{r^{(i)}_{1p} r^{(j)}_{pm}}{r^{(i)}_{1m}} \mathrm{e}^{\mathrm{i}k_p|x_j - x_i|}. \quad (16)$$

The quasibound states of an electron in the disordered Q1D or 2D systems can be found from the condition $\det(D^{(N)}_{i,j})_{M,1} = 0$. A particular case of this equation, the spectrum of the single δ-function scatterer ($N = 1$) with finite number of modes M in a 2D waveguide, was studied in [3]. Note that equation (16) reduces to the characteristic determinant of a purely 1D system (see [29, 30, 34]), if there is no coupling to the second, third, etc, mode, i.e. $r^{(p)}_{p1} = r^{(p)}_{1p} = 0$.

Inserting the appropriate GF's matrix elements, equation (13), $x = 1$ and $x' = x_N$, one can calculate the transmission amplitude $T^{(N)}_{nmL}$ of an electron through the system with N δ potentials. Similarly to $R^{(N)}_{nmL}$, we can write the explicit form of $T^{(N)}_{nmL}$ as a ratio of two determinants[3]

$$T^{(N)}_{nmL} = (-1)^N \frac{\mathrm{e}^{\mathrm{i}k_m(x_N - x_1)}}{\det(D^{(N)}_{i,j})_{M,1}} \times \begin{vmatrix} \delta_{nm} & r^{(1)}_{nm} & \cdots & r^{(N)}_{nm}\mathrm{e}^{\mathrm{i}k_n|x_N - x_1|} \\ 1 & \cdots & \cdots & \cdots \\ \vdots & \vdots & & (D^{(N)}_{i,j})_{M,m} \\ \mathrm{e}^{-\mathrm{i}k_m|x_N - x_1|} & \vdots & & \end{vmatrix}, \quad (17)$$

where the numerator of $T^{(N)}_{nmL}$ is obtained from the same determinant (16) by augmenting it on the left and on the top.

In the appendix we present the explicit expressions for the transmission and reflection amplitudes for the case when we have two δ functions ($N = 2$) and an arbitrary number of modes M.

Note that by employing equations (14) and (17), it is straightforward to check by mathematical induction that, for the scattering matrix elements, current conservation takes place:

$$\sum_{m=1}^{M} (T^{(N)}_{nmL} T^{(N)\,*}_{nmL} + R^{(N)}_{nmL} R^{(N)\,*}_{nmL}) = 1. \quad (18)$$

Here the summation is carried out over the propagating modes of the wire only.

Using the explicit forms of equations (14) and (17) it can be shown that the electron's transmission, $T^{(N)}_{nm}$, and reflection, $R^{(N)}_{nm}$, amplitudes in the limit of weak disorder are specifically given by

$$T^{(N)}_{mm} \approx \mathrm{e}^{\mathrm{i}k_m(x_N - x_1)} \frac{1 + \mathrm{i}\sum_{l=1}^{N} V_l \left(A_l - \frac{\sin^2\left(\frac{m\pi y_l}{L_t}\right)}{k_m L_t} \right)}{1 + \mathrm{i}\sum_{l=1}^{N} V_l A_l}, \quad (19)$$

[3] The phase factor $\mathrm{e}^{\mathrm{i}k_m(x_N - x_1)}$ in equation (17) was omitted in the analogous equation (10) of [22].

$$T^{(N)}_{nm} \approx -\frac{\mathrm{i}\mathrm{e}^{\mathrm{i}k_m(x_N - x_1)}}{L_t\sqrt{k_n k_m}} \sum_{l=1}^{N} V_l \sin\left(\frac{n\pi y_l}{L_t}\right) \times \sin\left(\frac{m\pi y_l}{L_t}\right) \mathrm{e}^{\mathrm{i}(k_n - k_m)(x_l - x_1)}, \quad (20)$$

$$R^{(N)}_{mm} \approx -\frac{\mathrm{i}}{L_t k_m} \sum_{l=1}^{N} V_l \sin^2\left(\frac{m\pi y_l}{L_t}\right) \mathrm{e}^{2\mathrm{i}(x_l - x_1)k_m}, \quad (21)$$

and

$$R^{(N)}_{nm} \approx -\frac{\mathrm{i}}{L_t\sqrt{k_n k_m}} \sum_{l=1}^{N} V_l \sin\left(\frac{n\pi y_l}{L_t}\right) \times \sin\left(\frac{m\pi y_l}{L_t}\right) \mathrm{e}^{\mathrm{i}(k_n + k_m)(x_l - x_1)} \quad (22)$$

with $A_l = \sum_{n=1}^{M} \sin^2(n\pi y_l/L_t)/L_t k_n$. y_l is the coordinate of the lth δ impurity in the y direction, and x_1 and x_N are the x coordinates of the first and last (Nth) δ functions. The wavenumbers k_n for the propagating modes are defined by equation (11). A finite number M includes effects from both the open and closed modes. The wavenumbers of the evanescent modes are obtained by setting $k_n = \mathrm{i}\kappa_n$, where κ is defined by equation (12).

The inverse localization length ξ_M as a function of the system size L and modes M is evaluated from

$$\xi_M^{-1} = -\lim_{L\to\infty} \frac{1}{2L} \left\langle \ln \sum_{n,m}^{M} |T^{(N)}_{nm}|^2 \right\rangle. \quad (23)$$

After ensemble averaging over the random potentials V_l, distributed uniformly in an interval $[-w/2, w/2]$ with the use of equations (19) and (20), equation (23) takes the simple form [22]

$$\frac{1}{\xi^{\delta}_M} = \frac{\alpha}{2NML_t^2} \sum_{l=1}^{N} \left\{ \sum_{n=1}^{M} \frac{\sin^2(\frac{n\pi y_l}{L_t})}{k_n} \right\}^2, \quad (24)$$

with $\alpha = \langle V_l^2 \rangle = w^2/12$. To derive equation (24) we first note that the phases in $T^{(N)}_{nm}$ are irrelevant for a white-noise potential where $\langle V_i V_k \rangle = \alpha\delta_{ik}$. In other words, the configuration of δ-potential atoms is not important for uncorrelated potentials, in the linear approximation of perturbation theory. This means that, without any loss of generality, we can arrange δ functions in the x direction periodically with spacing $a = 1$ and thus replace the finite length $L = Na$ by N. Next note that the above expression $1/\xi^{\delta}_M$ is exact to order w^2 for the weak disorder regime and valid for any type of distribution for y_l.

The expression (24) can be simplified further if we arrange δ functions periodically also in the y direction. This will be done in the next sections, separately for the situation when all the M channels are propagating and when ν are propagating and M–ν are evanescent.

3. Periodically arranged δ impurities

Let us consider the disordered strip model with the potential (2) in the form of periodically positioned 2D δ functions with random strength, V_l. For a 2D Kronig–Penney model with

vertical type of disorder in the distribution of scatterers the RLL Λ can be calculated analytically in the weak disorder regime using the characteristic determinant approach [22]. Note that a similar 2D strip model with δ-function potentials arranged periodically was used by Azbel and co-workers to investigate non-exponential-localized eigenstates in a disordered system [31, 35]. In numerical calculations of the persistent electron current in a disordered Q1D conducting ring with many channels, the analogous model to (2) with random positions and signs of δ potentials was adopted in [36].

Before entering into a more detailed analysis of this case, several assumptions are in order: (i) for simplicity we discuss the case when the spacing constants in the x and in the y directions are equal and are taken to be of unit length. This means that in the y direction we choose a discrete lattice whose points are located at $y_l = l$, $(l = 1, 2, \ldots, M)$ and thus the width $L_t = M+1$. (ii) In (i) the maximum value of l coincides with the number of propagating modes M. This is an essential point which allows us to consider the 2D δ-function strip model as a discrete lattice of size $(N \times M)$, where N and M are the number of δ potentials in the x and y directions, respectively. Equation (24) then simplifies to the following form:

$$\frac{M}{\xi_M^\delta(w)} = \frac{\alpha}{16(M+1)}\left[\sum_{n=1}^{M}\frac{3+\delta_{2n,M+1}}{k_n^2} + 2\sum_{n<p}^{M}\frac{2+\delta_{n+p,M+1}}{k_n k_p}\right]. \tag{25}$$

The structure of this formula for the inverse RLL is similar to the corresponding formula for the 2D Anderson TB model (see equation (34)), which justifies the similarity of the two models discussed in this paper.

Our task is now to evaluate equation (25) in the thermodynamic limit. As outlined above, in the case $\Lambda \ll 1$ the width L_t of the strip is much larger than $\xi_M(w)$. This means that, for large L_t (and hence for large M), the sums in equation (25) can be replaced by an integral and carried out by using the known formula (see, e.g., [37])

$$\sum_{n=0}^{M} f(n) = \int_{-\frac{1}{2}}^{M+\frac{1}{2}} f(n)\,\mathrm{d}n - \tfrac{1}{24}\left[f'\left(M+\tfrac{1}{2}\right) - f'\left(-\tfrac{1}{2}\right)\right]. \tag{26}$$

This enables us to obtain an approximate analytical expression for equation (25) when $\Lambda \ll 1$. Performing the integrals and keeping only the relevant terms, after some algebra, the following formula for the inverse RLL $1/\Lambda^\delta = M/\xi_M^\delta$, equation (25), is obtained (from here on, we substitute M for L_t as the width of the strip):

$$\frac{1}{\Lambda^\delta} = C^\delta + \frac{M}{\xi_\infty^\delta(w)}, \tag{27}$$

where

$$C^\delta = \frac{b\alpha}{8\pi^2}\left(\arcsin b - \frac{5}{8}\ln\frac{1+b}{1-b}\right) \tag{28}$$

and $b \equiv \pi/\sqrt{E_\mathrm{F}}$. ξ_∞^δ is the localization length in the infinitely large system in the limit $M \to \infty$ and can be determined as

$$\xi_\infty^\delta = \lim_{M\to\infty}\xi_M^\delta \approx \frac{8\pi^2}{\alpha(\arcsin b)^2}. \tag{29}$$

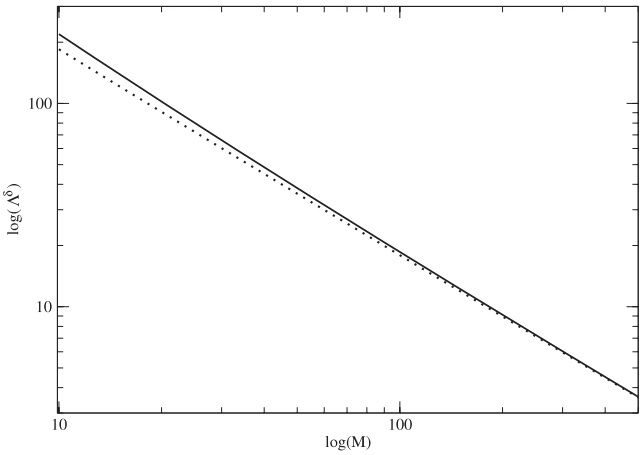

Figure 1. Log–log plot of the renormalized localization length Λ^δ as a function of modes M for the values of the Fermi energy $E_\mathrm{F} = 10$ and for disorder $w = 0.5$. Solid and dashed lines are given by equations (25) and (27), respectively, and the slope of the solid straight line is equal to -1.

Equation (27) with equation (36) (see below) represent the central results of this work. They express the RLL in terms of number of modes M and disorder w and show that $1/\Lambda^\delta$ increases linearly with increasing number M of δ potentials in the y direction. This indicates that in a 2D disordered system of δ potentials localization sets in for an arbitrarily small disorder $\alpha = w^2/12$, as predicted [23].

It is worth noticing that an expression similar to equation (27) was found in [19] using a numerical estimate of the β function in 2D systems with spin–orbit coupling in the insulating phase, where the disorder is very strong and the localization length is short. Thus $\xi_M^\delta(w) \ll M$, i.e. the inequality $\Lambda^\delta \ll 1$ holds, and thus spin–orbit coupling does not play any essential role in the insulating phase. In [19] C^δ and $\xi_\infty(w)$ were parameters fitted at each disorder w (or α).

In figure 1 we have plotted the Λ^δ, equation (25), as a function of the number of modes M for the values of the Fermi energy $E_\mathrm{F} = 10$ $(b = 0.99)$ and of the disorder $w = 0.5$. The slope of the solid straight line is equal -1, as expected. We have checked that for large values of M the dashed line, i.e. the approximate analytical expression (27) agrees very well with the exact expression (25) in the whole range $0 < b < 1$. The deviation between the two lines for small M in figure 1 depends on the specific value of the logarithmic term in C^δ.

In figure 2 the dependence of $\ln\xi_\infty^\delta$ is shown as a function of the disorder parameter w (or α). One can see that the curve is consistent with the numerical result of [24] for the 2D strip model. Note that ξ_∞^δ increases with increasing E_F (i.e. b is decreasing) and decreases with increasing disorder α of the system. In the limit of large E_F (b tends to zero) we have

$$\xi_\infty^\delta = \frac{8E_\mathrm{F}}{\alpha} \tag{30}$$

which agrees with the well-known result of LL in the 1D system [38].

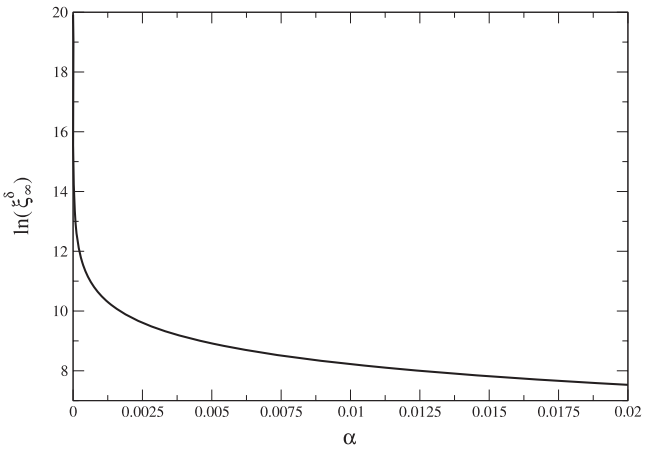

Figure 2. Dependence of the localization length on disorder, $\alpha = w^2/12$, in the infinitely large system based on equation (29).

3.1. RLL and evanescent modes

Our objective in this section is to extend our previous calculations [22] and to investigate the influence of evanescent states on the scaling behavior of RLL. We proceed along the same lines as in section 3 and we show that only minor modifications of the final expression for the RLL, equation (25) are required in order to include (M–ν) evanescent modes. The final expression for RLL can be presented in the following form:

$$\frac{\nu}{\xi^{\delta}_{\nu}(M,w)} = \frac{\alpha}{16(M+1)}\left[\sum_{n=1}^{\nu}\frac{3+\delta_{2n,M+1}}{k_n^2} + 2\sum_{n<p}^{\nu}\frac{2+\delta_{n+p,M+1}}{k_n k_p}\right], \tag{31}$$

where ν is the number of propagating modes and M is the total number of modes (propagating and evanescent). From the comparison of RLL in the presence of evanescent modes, equation (31), with the expression of RLL when evanescent modes are absent (see equation (25)) one can see that in equation (31) the sum runs only up to ν propagating modes. The reason for this restriction in such a simple way was pointed out by Heinrichs [10], in the analysis of the effect evanescent states have on the ensemble average conductance in coupled two- and three-chain TB model for weak disorder. The main idea is that the absence of coupling effects between propagating and evanescent modes is specific to the weak disorder approximation, where first-order perturbation was used, which ignores higher-order coupling effects. A similar situation arises also during the calculation of RLL in multi-channel 2D δ-potential disordered systems with M–ν evanescent modes in the weak disordered regime, as follows from equation (31).

It is not difficult to see from (31) that the presence of evanescent modes enhances the RLL (the localization length expressed in units of the strip length) with respect to RLL when evanescent modes are absent (see equation (25)). The reason is quite clear from a physical point of view: with increasing numbers of evanescent modes, the δ-type scatterer becomes more and more transparent. As the number of evanescent modes increases towards infinity, we get perfect transmission for all the values of the Fermi energy [2, 13, 25]. This leads to perfect conductance and hence to the increase in localization length. The main consequence of enhanced RLL in a 2D strip is the fact that the presence of M–ν evanescent modes qualitatively changes the limiting behavior of the single parameter scaling hypothesis for small Λ: in the limit $\Lambda \to 0$ β tends to -2, instead of -1 (details of the analytical derivation will be given elsewhere [44]).

Similarly to equation (27), we derive an approximate expression for $\nu/\xi^{\delta}_{\nu}(M,w)$, equation (31), for large ν:

$$\frac{1}{\Lambda^{\delta}_{\nu}} = C^{\delta} + \frac{\nu^2}{M\xi^{\delta}_{\infty}(w)}, \tag{32}$$

where the parameters C^{δ} and ξ^{δ}_{∞} are defined by equations (28) and (29), respectively. Using this expression and equation (27), it is easy to see that inequality $\Lambda^{\delta}/\Lambda^{\delta}_{\nu} < 1$ takes place:

$$\frac{\Lambda^{\delta}}{\Lambda^{\delta}_{\nu}} = \frac{C^{\delta} + \frac{\nu^2}{M\xi^{\delta}_{\infty}(w)}}{C^{\delta} + \frac{M}{\xi^{\delta}_{\infty}(w)}} < 1. \tag{33}$$

4. Tight-binding model

In this section we consider the 2D TB model with arbitrary number M of modes and finite length N for which the LL was calculated in [22] in the weak disordered regime:

$$\frac{M}{\xi^{\mathrm{TB}}_{M}(w)} = \frac{\alpha}{16(M+1)} \times \left[\sum_{n=1}^{M}\frac{3+\delta_{2n,M+1}}{\sin^2 k_n} + 2\sum_{n<p}^{M}\frac{2+\delta_{n+p,M+1}}{\sin k_n \sin k_p}\right], \tag{34}$$

where α is the same as in the model of 2D δ-function potentials, equation (25). The wavevector k_n must be found from the dispersion relation [39, 40]

$$E = 2\cos k_n + 2t\cos\frac{n\pi}{M+1}. \tag{35}$$

It is easy to check that, for particular values $M = 2$ or 3, the results of [5] for LL can be reproduced from equation (34). In the limit of no interchain hopping ($t = 0$ and thus all k_n are equal) the same equation reduces precisely to the 1D result for LL [38]: $\xi^{\mathrm{TB}}_{1}(w) = (8\sin^2 k)/\alpha$, as expected.

At the band center ($E = 0$) and proceeding along the same lines as in section 3.1, we can evaluate the sums in equation (34) by replacing them by integrals and evaluating them using equation (26) in the case $\Lambda \ll 1$. After some algebra, the following formula for the inverse RLL M/ξ^{δ}_{M}, equation (34), is obtained:

$$\frac{1}{\Lambda^{\mathrm{TB}}} = C^{\mathrm{TB}} + \frac{M}{\xi^{\mathrm{TB}}_{\infty}(w)}, \tag{36}$$

where

$$C^{\mathrm{TB}} = \frac{\alpha}{8\pi(1-t^2)}\left[F\left(\pi, -\frac{t^2}{1-t^2}\right) - \frac{3\pi\sqrt{1-t^2}}{2}\right] \tag{37}$$

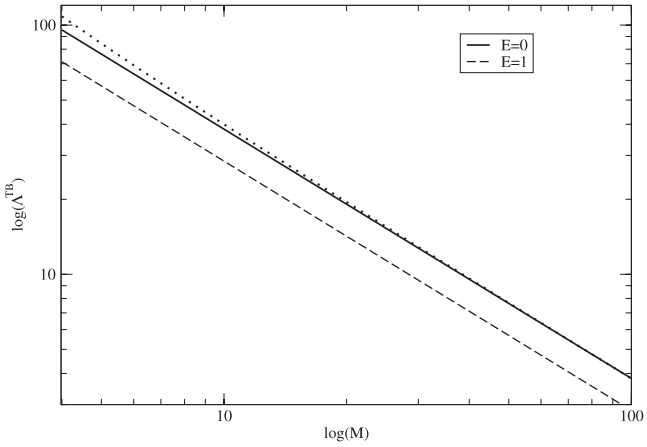

Figure 3. Log–log plot of the renormalized localization length Λ^{TB} as a function of modes M at the band center $E = 0$ (solid and dotted lines) and at $E = 1$ (dashed line). The value of disorder is $w = 0.5$ and the interchain hopping is $t = 0.5$. The solid and dotted lines are given by equations (34) and (36), respectively. For $E = 1$ the dashed line was calculated from equation (34). All the channels are propagating.

and $F(\phi, m)$ is the elliptic integral of the first kind. ξ_∞^{TB} is the localization length of an infinitely large system TB model at the band center $E = 0$ and defined by

$$\xi_\infty^{\mathrm{TB}} = \lim_{M\to\infty} \xi_M^{\mathrm{TB}} \approx \frac{8\pi^2(1-t^2)}{\alpha F^2(\pi, -\frac{t^2}{1-t^2})}. \tag{38}$$

A similar expression for Λ^{TB} at $E > 0$, in the form of the elliptic integral (of the first kind), can be found in [16], where the authors used a perturbative formula for the lowest Lyapunov exponent of an Anderson model on a strip.

Using the series expansion for $F(\phi, m) \approx \phi$ when $\phi^2 m/6 \ll 1$ (in terms of t, the latter inequality is: $t^2 \ll 6/(\pi^2+6)$), one can get an approximate expression for $\xi_\infty^{\mathrm{TB}} \approx 8/\alpha$, which is Thouless' expression for localization length $(8\sin^2 k)/\alpha$ at $k = \pi/2$.

In figure 3 we represent the Λ^{TB}, equation (34), as a function of the number of modes M at the band center $E = 0$ (solid line) and at $E = 1$ (dashed line) on a double logarithmic scale. The value of disorder is $w = 0.5$ and the interchain hopping is $t = 0.5$. Although for $E = 1$ the RRL (dashed line) is decreasing the slopes of the lines, presented in figure 3, are -1, as expected. One can see that the approximate analytical expression (36) (dotted line) agrees very well with the exact expression (34) for large values of the modes M. We have checked that good agreement is found for both dotted and solid lines also in the range of hopping parameter $0 < t \leqslant 0.8$

4.1. Mean free path in disordered multi-channel TB modes

In [10], the author discussed the influence of evanescent modes on localization length, $\xi_M^{\mathrm{TB}}(w)$, in few-channel ($M = 2, 3$) strips, as described by the standard Anderson TB model. Using a scattering matrix approach and the expression for the single elastic mean free path l, defined in the framework of a maximum entropy approach to multi-channel systems [41], it was shown that for the two- and three-channel cases the following relation holds between localization length $\xi_M^{\mathrm{TB}}(w)$ and l:

$$\xi_M^{\mathrm{TB}}(w) = 2l. \tag{39}$$

This result agrees with the result for 1D conductors and demonstrates that all states are localized in two- and three-chain disordered systems. On the other hand, if we extrapolate the above relation to the many-channel case then even for very large M and for weak disorder all states must be localized. Furthermore, there is no length scale that leads to the metallic Ohm's law for conductance. This is in contrast to the well-known Thouless' relation [38]:

$$\xi_M^{\mathrm{TB}}(w) \approx Ml, \tag{40}$$

which shows that there must be a domain of length scales where the eigenstates are delocalized (diffusive quasimetallic domain) (see, e.g., [42]). The physical origin of this discrepancy, as pointed out by Heinrichs in [43], is that in the case of the multi-channel TB strip model the mean free paths in the conducting channels are generally different. Thus one must, instead of using the concept of the single elastic mean free path [41], use the following definition for the average mean free path $l_M^{\mathrm{TB}}(w)$:

$$\frac{1}{l_M} = \frac{1}{N}\sum_{n,m=1}^{M} \langle |R_{nm}^{(N)}|^2 \rangle. \tag{41}$$

We recall that $R_{nm}^{(N)}$ is a reflection amplitude for an electron, which is incident along the nth transverse mode and scattered back along the mth transverse mode as given by (22).

The difference between $1/l_M$, equation (41), and the expression $1/l$, equation (39), used in the maximum entropy approach (see, e.g., [10]) is that the latter contains an additional factor $1/M$. Taking into account the correct relation, $l = Ml_M$, equation (39) now is [43]

$$\xi_M^{\mathrm{TB}}(w) = 2Ml_M, \qquad M = 2, 3. \tag{42}$$

The existence of the metallic domain in the coupled disordered two and three TB chains follows from this equation.

Below we generalize relation (42) for an arbitrary number of TB channels M using the definition for the average mean free path (41). We discuss the two cases when all M channels are propagating and for (M–ν) evanescent channels.

4.1.1. All channels are propagating. As mentioned in section 1, one can discuss two different models for a disordered 2D system within the framework of the same approach: a set of 2D δ potentials with signs and strengths determined randomly and a TB Hamiltonian with several modes and on-site disorder.

We will use equations (19)–(22) to calculate the transmission and reflection coefficients in a TB model, and hence the average mean free path l_M, equation (41). By replacing k_n by $\sin k_n$ in these expressions and averaging over the disorder we obtain for $\langle |T_{nm}^{(N)}|^2 \rangle$ and $\langle |R_{nm}^{(N)}|^2 \rangle$ the following expressions [44].

If $2m \neq M+1$:

$$\langle|T^{(N)}_{mm}|^2\rangle = 1 - \frac{N\alpha}{8(M+1)} \times \left\{\frac{3}{\sin^2 k_m} + \frac{2}{\sin k_m}\sum_{m\neq p}^{M}\frac{2+\delta_{m+p,M+1}}{\sin k_p}\right\}. \quad (43)$$

If $2m = M+1$, then

$$\langle|T^{(N)}_{mm}|^2\rangle = 1 - \frac{N\alpha}{2(M+1)}\left\{\frac{1}{\sin^2 k_m} + \frac{1}{\sin k_m}\sum_{m\neq p}^{M}\frac{1}{\sin k_p}\right\}, \quad (44)$$

or

$$\langle|T^{(N)}_{nm}|^2\rangle = \frac{N\alpha}{8(M+1)}\frac{2+\delta_{m+n,M+1}}{\sin k_m \sin k_n}. \quad (45)$$

$$\langle|R^{(N)}_{mm}|^2\rangle = \frac{N\alpha}{8(M+1)}\frac{3+\delta_{2m,M+1}}{\sin^2 k_m}, \quad (46)$$

or

$$\langle|R^{(N)}_{nm}|^2\rangle = \frac{N\alpha}{8(M+1)}\frac{2+\delta_{m+n,M+1}}{\sin k_n \sin k_m}. \quad (47)$$

Inserting equations (46) and (47) in equation (41), we get for the average mean free path

$$\frac{1}{l_M} = \frac{\alpha}{8(M+1)}\left[\sum_{n=1}^{M}\frac{3+\delta_{2n,M+1}}{\sin^2 k_n} + 2\sum_{n<p}^{M}\frac{2+\delta_{n+p,M+1}}{\sin k_n \sin k_p}\right]. \quad (48)$$

Comparison of equation (48) with the expression for $M/\xi^{\mathrm{TB}}_M(w)$, equation (34), yields the desired result:

$$\xi^{\mathrm{TB}}_M(w) = 2Ml_M, \qquad M = 2, 3\ldots \quad (49)$$

which is the natural generalization of equation (42) for an arbitrary number of channels M and is exact to order w^2 for the weak disordered regime. Equation (49) is comparable with the result of [45], $\xi_M(w) = l_c(2M+1)$, where l_c is the elastic scattering length.

The range of length scales for the diffusive quasimetallic domain, where Ohm's law for the conductance can be observed, is

$$l_M \ll l \ll Ml_M = \xi^{\mathrm{TB}}_M(w). \quad (50)$$

4.1.2. Mean free path: $(M-\nu)$ evanescent channels. Consider the case of $E_1 < E_2 \cdots E < E_\nu$. Only the first ν modes can propagate along the 2D system, whereas M–ν cannot (M is the total number of channels). The influence of evanescent modes on the calculation of the free path can be treated similarly to sections 2 and 3. All the steps can be repeated for this case in a TB model. We obtain the final expressions for the inverse localization length and for an average mean free path

$$\frac{\nu}{\xi_\nu} = \frac{\alpha}{16(M+1)}\left[\sum_{n=1}^{\nu}\frac{3+\delta_{2n,M+1}}{\sin^2 k_n} + 2\sum_{n<p}^{\nu}\frac{2+\delta_{n+p,M+1}}{\sin k_n \sin k_p}\right], \quad (51)$$

and

$$\frac{1}{l_\nu} = \frac{\alpha}{8(M+1)}\left[\sum_{n=1}^{\nu}\frac{3+\delta_{2n,M+1}}{\sin^2 k_n} + 2\sum_{n<p}^{\nu}\frac{2+\delta_{n+p,M+1}}{\sin k_n \sin k_p}\right]. \quad (52)$$

It is useful to compare the pair of equations (51) and (52) with (34) and (48). Their similarity is obvious. The essential difference is that the index n in the summation runs up to ν, i.e. up to the maximum propagating mode. The use of the weak disorder approximation leads to the suppression of the effect of $(M-\nu)$ evanescent modes, and was discussed in section 3 in connection with the 2D δ-potential strip model (see also [10]). The presence of evanescent modes enhances the localization length (hence the average mean free path) in the TB model, similar to the 2D δ-function strip model. The final result is (compare with equation (49))

$$\xi^{\mathrm{TB}}_\nu(w) = 2\nu l_\nu. \quad (53)$$

It is worthwhile to note that the factor 2 which appears in equations (49) and (53) is the consequence of the weak disorder approximation used in the present paper. Indeed, it follows from current conservation in an M-channel system that

$$\sum_{n,m}^{M}\langle|T^{(N)}_{nm}|^2\rangle = M - \sum_{n,m}^{M}\langle|R^{(N)}_{nm}|^2\rangle, \quad (54)$$

which can be easily verified by using the explicit expressions for the scattering matrix elements, equations (43)–(47), calculated in the weak disorder approximation. By expanding (23) to lowest order of the powers of the disorder and, after averaging over realizations using the model for an uncorrelated potential $\langle\epsilon_i\epsilon_k\rangle = \epsilon_0^2\delta_{ik}$, one can show that the inverse of the localization length, for sufficiently large L, is

$$\frac{1}{\xi^{\mathrm{TB}}_M} = \frac{1}{2NM}\sum_{n,m=1}^{M}\langle|R^{(N)}_{nm}|^2\rangle \equiv \frac{1}{2Ml_M}. \quad (55)$$

In deriving the first equality we used the fact that in the weak disordered limit in Q1D systems the well-known relationship between the various localization lengths takes place, namely $\langle\ln T\rangle = \frac{1}{2}\ln\langle T\rangle$ (see, e.g., [9]). The latter equality in equation (55) follows from the definition of the average mean free path, equation (41).

Concluding this section let us note that influence of the evanescent modes on localization length of the Q1D system was also discussed in [15, 16], based on evaluation of the double stochastic matrix, the size of which is proportional to the strip width.

5. Summary

We consider two different models, mentioned in the Introduction, which are appropriate for disordered mesoscopic systems: (1) the δ-function potentials and (2) constant nearest-neighbor coupling multichain tight-binding Anderson models. They can be discussed within the framework of the same approach. The general structure of electron scattering matrix elements, the localization length and the average mean free path in multi-channel systems are model-independent in both models. To switch from a δ-potential model to a TB model one must change the strength of the δ potential V_l by the diagonal energy in the TB model and use the unperturbed GF for each

case (see the appendix). We study the influence of evanescent modes on the scaling behavior of the renormalized localization length in both systems. We perform an analytical calculation of the renormalized localization lengths for large numbers of modes M, equations (27) and (36), for both models. We also derive the localization lengths in the thermodynamic limit in both models. We show that the presence of evanescent modes enhances the RLL, (32), with respect to the value obtained when evanescent modes are absent (27). We also derive an exact relation between the localization length and the corresponding average mean free path for M-channel systems when evanescent modes are present.

Acknowledgments

AS acknowledges a grant from International Exchange Office of TUS. VG wishes to acknowledge the kind hospitality of the Physics Departments of TUS for the stay, during which the final part of this work was completed. VG thanks M Ortuño, T Meyer and J Talamantes for critical reading of the manuscript and for many useful comments that helped to improve the paper. Special thanks to E Jódar for preparing the figures. The work was partially sponsored by FEDER and the Spanish DGI under project no. FIS2007-62238.

Appendix. 2D strip model with 2δ potentials and M propagating modes

A.1. Incident from the left

Consider the strip model with two δ-function potentials located at (x_1, y_1) and (x_2, y_2). An electron is incident from the left onto the system. According to the general expression $T^{(N)}_{nmL}$, equation (17), the amplitude of transmission in terms of the single δ-function reflection amplitude, $r^{(l)}_{nm}$ ($l = 1, 2$), is

$$T^{(2)}_{nmL} = \frac{\mathrm{e}^{\mathrm{i}k_m a_1}}{\det(D^{(2)}_{i,j})_{M,1}} \times \begin{vmatrix} \delta_{nm} & r^{(1)}_{nm} & r^{(2)}_{nm}\mathrm{e}^{\mathrm{i}k_n a_1} \\ 1 & -1 & \dfrac{\sum_{p=1}^{M} r^{(1)}_{1p} r^{(2)}_{pm}\mathrm{e}^{\mathrm{i}k_p a_1}}{r^{(1)}_{1m}} \\ \mathrm{e}^{-\mathrm{i}k_m a_1} & \dfrac{\sum_{p=1}^{M} r^{(2)}_{1p} r^{(1)}_{pm}\mathrm{e}^{\mathrm{i}k_p a_1}}{r^{(2)}_{1m}} & -1 \end{vmatrix}, \tag{56}$$

where $r^{(l)}_{nm}$ is defined by equation (15), the wavenumber k_l by (11) and $a_1 = x_2 - x_1$. In the expression above, all k_l are real quantities. If the lth mode is evanescent, then $k_l = \mathrm{i}\kappa_l$ with κ_l is defined by (12). The denominator $\det(D^{(2)}_{i,j})_{M,1}$ in equation (56), based on the definition, (16), in this case is

$$\det(D^{(2)}_{i,j})_{M,1} = \begin{vmatrix} -1 & \dfrac{\sum_{p=1}^{M} r^{(1)}_{1p} r^{(2)}_{pm}\mathrm{e}^{\mathrm{i}k_p a_1}}{r^{(1)}_{1m}} \\ \dfrac{\sum_{p=1}^{M} r^{(2)}_{1p} r^{(1)}_{pm}\mathrm{e}^{\mathrm{i}k_p a_1}}{r^{(2)}_{1m}} & -1 \end{vmatrix}. \tag{57}$$

The reflection amplitude $R^{(N)}_{nmL}$ follows from equation (14) and is given by

$$R^{(2)}_{nmL} = \frac{1}{\det(D^{(2)}_{i,j})_{M,1}} \times \begin{vmatrix} 0 & r^{(1)}_{nm} & r^{(2)}_{nm}\mathrm{e}^{\mathrm{i}k_n a_1} \\ 1 & -1 & \dfrac{\sum_{p=1}^{M} r^{(1)}_{1p} r^{(2)}_{pm}\mathrm{e}^{\mathrm{i}k_p a_1}}{r^{(1)}_{1m}} \\ \mathrm{e}^{\mathrm{i}k_m a_1} & \dfrac{\sum_{p=1}^{M} r^{(2)}_{1p} r^{(1)}_{pm}\mathrm{e}^{\mathrm{i}k_p a_1}}{r^{(2)}_{1m}} & -1 \end{vmatrix}. \tag{58}$$

It can be verified directly that equation (56) for the case of two modes ($M = 2$) leads to ($n = m = 1$)

$$\begin{aligned} T^{(2)}_{11} = {} & \mathrm{e}^{\mathrm{i}k_1 a_1}[(1 + r^{(1)}_{11})(1 + r^{(2)}_{11}) + r^{(1)}_{12} r^{(2)}_{21}\mathrm{e}^{\mathrm{i}(k_2 - k_1)a_1} \\ & - r^{(1)}_{22} r^{(2)}_{22}\mathrm{e}^{2\mathrm{i}k_2 a_1} - \mathrm{e}^{\mathrm{i}(k_1 + k_2)a_1} r^{(2)}_{12} r^{(1)}_{21}] \\ & \times [1 - r^{(1)}_{11} r^{(2)}_{11}\mathrm{e}^{2\mathrm{i}k_1 a_1} - r^{(1)}_{22} r^{(2)}_{22}\mathrm{e}^{2\mathrm{i}k_2 a_1} \\ & - (r^{(1)}_{12} r^{(2)}_{21} + r^{(1)}_{21} r^{(2)}_{12})\mathrm{e}^{\mathrm{i}(k_1 + k_2)a_1}]^{-1}, \end{aligned} \tag{59}$$

which coincides with the expression of $T^{(2)}_{11}$ calculated by the transfer matrix method in [26] after the notation is adjusted appropriately. The rest of the scattering matrix elements for this case can easily be calculated from the above explicit expressions.

A.2. Incident from the right

Using the procedure outlined in section 2, we can similarly derive the expressions for the reflection and transmission amplitudes for electrons incident from the right. The only difference now is that we must isolate the term corresponding to the points on the left-hand edge x_1, x_2, etc. The expressions for the scattering matrix elements from the right are very similar to equations (14) and (17). The essential difference is that the numerators of $R^{(N)}_{nmR}$ and $T^{(N)}_{nmR}$ now are obtained from the same determinant (16) by augmenting it on the right and on the bottom. The transmission $T^{(N)}_{nmR}$ and reflection $R^{(N)}_{nmR}$ amplitudes are, respectively,

$$T^{(2)}_{nmR} = \frac{\mathrm{e}^{\mathrm{i}k_m a_1}}{\det(D^{(2)}_{i,j})_{M,1}} \times \begin{vmatrix} -1 & \dfrac{\sum_{p=1}^{M} r^{(1)}_{1p} r^{(2)}_{pm}\mathrm{e}^{\mathrm{i}k_p a_1}}{r^{(1)}_{1m}} & \mathrm{e}^{-\mathrm{i}k_m a_1} \\ \dfrac{\sum_{p=1}^{M} r^{(2)}_{1p} r^{(1)}_{pm}\mathrm{e}^{\mathrm{i}k_p a_1}}{r^{(2)}_{1m}} & -1 & 1 \\ r^{(1)}_{nm}\mathrm{e}^{\mathrm{i}k_n a_1} & r^{(2)}_{nm} & \delta_{nm} \end{vmatrix}, \tag{60}$$

$$R^{(2)}_{nmR} = \frac{1}{\det(D^{(2)}_{i,j})_{M,1}} \times \begin{vmatrix} -1 & \dfrac{\sum_{p=1}^{M} r^{(1)}_{1p} r^{(2)}_{pm}\mathrm{e}^{\mathrm{i}k_p a_1}}{r^{(1)}_{1m}} & \mathrm{e}^{\mathrm{i}k_m a_1} \\ \dfrac{\sum_{p=1}^{M} r^{(2)}_{1p} r^{(1)}_{pm}\mathrm{e}^{\mathrm{i}k_p a_1}}{r^{(2)}_{1m}} & -1 & 1 \\ r^{(1)}_{nm}\mathrm{e}^{\mathrm{i}k_n a_1} & r^{(2)}_{nm} & 0 \end{vmatrix}. \tag{61}$$

Finally, we note that the expressions for $T^{(N)}_{nm}$ and $R^{(N)}_{nm}$ for a left- and right-incident electron in the TB model are obtained by replacing the unperturbed GF for normal mode n (see equation (10)):

$$G^0_n(x, x') = -\frac{\mathrm{i}}{2k_n}\mathrm{e}^{\mathrm{i}k_n|x - x'|}$$

by the appropriate GF for the TB model [39, 40]:

$$G_n^0(m,l) = -\frac{\mathrm{i}}{2\sin q_n}\mathrm{e}^{-\mathrm{i}q_n|m-l|}. \tag{62}$$

The wavevector k_n is given by equation (11) and q_n is defined by equation (35). The similarity between these two methods was demonstrated in [46], where the authors studied the density of states, the distribution of energy spacings and the transmission coefficients of 1D quasiperiodic Fibonacci and Thue–Morse systems using the zeros of the characteristic determinants equation (16).

References

[1] Cahay M, Mclennan M and Datta S 1988 *Phys. Rev.* B **37** 10125
[2] Bagwell P F 1990 *J. Phys.: Condens. Matter* **2** 6179
[3] Boese D, Lischka M and Reichl L E 2000 *Phys. Rev.* B **61** 5632
[4] Souma S and Suzuki A 2002 *Phys. Rev.* B **65** 115307
[5] Heinrichs J 2002 *Phys. Rev.* B **66** 155434
[6] Cattepan G and Maglione E 2003 *Am. J. Phys.* **71** 903
[7] Faist J, Gueret P and Rothizen H 1990 *Phys. Rev.* B **42** 3217
[8] Gurvitz S A and Levinson Y B 1993 *Phys. Rev.* B **47** 10578
[9] Cahay M, Bandyopadhyay S, Osman M A and Grubin H L 1990 *Surf. Sci.* **228** 301
[10] Heinrichs J 2003 *Phys. Rev.* B **68** 155403
[11] Ben-Aryeh Y 2008 *Appl. Phys.* B **91** 157
[12] Freilikher V, Liansky B A, Yurkevich I, Maradudin A A and McGurn A R 1997 *Phys. Rev.* E **51** 6301
[13] Deo P S 2007 *Phys. Rev.* B **75** 235330
[14] Serra L, Sanchez D and Lopez R 2007 *Phys. Rev.* B **76** 045339
[15] Schulz-Baldes H 2004 *Geom. Funct. Anal.* **14** 1089
[16] Römer R A and Schulz-Baldes H 2004 *Europhys. Lett.* **68** 247–53
[17] Cuevas E 1999 *Phys. Rev. Lett.* **83** 140
[18] Prior J, Somoza A M and Ortuño M 2005 *Phys. Rev.* B **72** 024206
[19] Asada Y, Slevin K and Ohtsuki T 2004 *Phys. Rev.* B **70** 035115
[20] Beenakker C W J 1997 *Rev. Mod. Phys.* **69** 731
[21] Janssen M 1998 *Phys. Rep.* **295** 1
[22] Gasparian V 2008 *Phys. Rev.* B **77** 113105
[23] Abrahams E, Anderson P W, Licciardello D C and Ramakrishnan T V 1979 *Phys. Rev. Lett.* **42** 673
[24] MacKinnon A and Kramer B 1983 *Z. Phys.* B **53** 1
[25] Vargimaidis V and Polatoghlu M 2003 *Phys. Rev.* B **67** 245303
[26] Kumar A and Bagwell P F 1991 *Phys. Rev.* B **43** 9012
[27] Gasparian V M, Altshuler B L, Aronov A G and Kasamanian Z H 1988 *Phys. Lett.* A **132** 201
[28] Aronov A G, Gasparian V and Gummich U 1991 *J. Phys.: Condens. Matter* **3** 3023
[29] Gasparian V and Khachatrian A 1993 *Solid State Commun.* **85** 1061
[30] Grosche S 1993 *Ann. Phys., Lpz.* **2** 557
[31] Goda M, Azbel M and Yamada H 1999 *Int. J. Mod. Phys.* B **13** 2705 and references therein
[32] Babikov V V 1988 *Metod Fazovykh Funktsii v Kvantovoi Mekhanike* (Moscow: Nauka)
[33] Fisher D S and Lee P A 1981 *Phys. Rev.* B **23** 6851
[34] Gasparian V 1989 *Fiz. Tverd. Tella* **31** 162
Gasparian V 1989 *Sov. Phys. Solid State* **31** 266 (Engl. Transl.)
[35] Goda M, Azbel M and Yamada H 2001 *Physica* B **296** 66
[36] Feilhauer J and Mosko M 2001 *Physica* E **40** 1582
[37] Abrikosov A A 1988 *Fundamentals of the Theory of Metals* (Amsterdam: North-Holland)
[38] Thouless D J 1977 *Phys. Rev. Lett.* **39** 1167
[39] Economou E N 1983 *Green's Functions in Quantum Physics* (Berlin: Springer)
[40] Ruiz J, Jódar E and Gasparian V 2007 *Phys. Rev.* B **75** 235123
[41] Mello P A, Pereyra P and Kumar N 1988 *Ann. Phys. NY* **181** 290
[42] Imry Y 1997 *Introduction to Mesoscopic Physics* (New York: Oxford University Press)
[43] Heinrichs J 2007 *Phys. Rev.* B **76** 033305
[44] Cahay M *et al* unpublished
[45] Macedo A M S and Chalker J T 1992 *Phys. Rev.* B **46** 14985
[46] Carpena P, Gasparian V and Ortuño M 1995 *Phys. Rev.* B **51** 12813